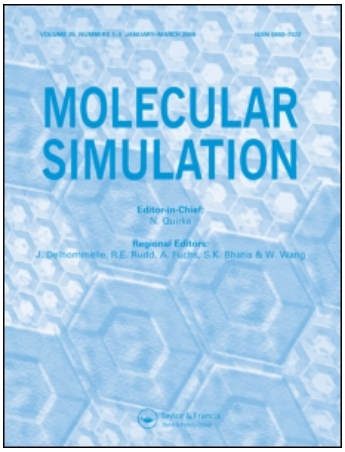

Molecular Simulation
Publication details, including instructions for authors and subscription information:
http://www.informaworld.com/smpp/title~content=t713644482

Density functional studies on copper-catalysed asymmetric aziridination of diazoacetate with imines

Fen Wang[a]; Qingxi Meng[b]; Ming Li[c]
[a] Department of Chemistry, Taishan University, Taian, Shandong, People's Republic of China [b] Department of Chemistry and Material Science, Shandong Agricultural University, Taian, Shandong, People's Republic of China [c] Department of Chemistry, Southwest University, Chongqing, People's Republic of China

First published on: 29 July 2009

To cite this Article Wang, Fen , Meng, Qingxi and Li, Ming(2010) 'Density functional studies on copper-catalysed asymmetric aziridination of diazoacetate with imines', Molecular Simulation, 36: 1, 15 — 25, First published on: 29 July 2009 (iFirst)
To link to this Article: DOI: 10.1080/08927020903096056
URL: http://dx.doi.org/10.1080/08927020903096056

Molecular Simulation
Vol. 36, No. 1, January 2010, 15–25

Taylor & Francis
Taylor & Francis Group

Density functional studies on copper-catalysed asymmetric aziridination of diazoacetate with imines

Fen Wang[a], Qingxi Meng[b]* and Ming Li[c]

[a]*Department of Chemistry, Taishan University, Taian, Shandong 271021, People's Republic of China;* [b]*Department of Chemistry and Material Science, Shandong Agricultural University, Taian, Shandong 271018, People's Republic of China;* [c]*Department of Chemistry, Southwest University, Chongqing 400715, People's Republic of China*

(*Received 17 February 2009; final version received 30 May 2009*)

Density functional theory has been used to study copper(I)-catalysed aziridination of diazoacetate with imines. All the intermediates and the transition states were optimised completely at B3LYP/6-31G(d) level. Calculation results confirm that copper(I)-catalysed aziridination of diazoacetate with imines is exothermic, and the total released Gibbs free energy is about −170 kJ/mol. Copper(I)-catalysed aziridination has two reaction modes: I and II, and thus the reaction mode I is dominant. The formation of the copper(I)–carbene–imine complex **M3** (i.e. the attack of imines on copper–carbon(carbene) of copper–carbene intermediate **M2**) is the rate-determining step and the chirality-limiting step for copper-catalysed asymmetric aziridination. The reaction channel **CA2 → M1a → TS1a → M2 → TS2a2 → M3a2 → TS3a2 → M4a2 → → TS1a → M2 → TS2a2 → M3a2 → TS3a2 → M4a2 → P1** is the most favourable one. The dominant products predicted theoretically are of (*R*)-chirality.

Keywords: chiral bisoxazoline–copper(I) complex; aziridination; imines; reaction mechanism; DFT

1. Introduction

Aziridines have been attractive organic molecules due to their great synthetic utilities [1–3]. Aziridines have been used as intermediates in the preparation of amino acids [4–5], β-lactams [6], polymers [7] and pyrrolidines [8]. A number of synthetic aziridines have found biological applications as antitumour agents, antibiotics and as enzyme inhibitors [9]. Several naturally occurring aziridines have been shown to exhibit antibiotic and antitumour activity [9]. Many non-catalytic pathways to aziridines have been developed [10,11]; recently however, the development of the asymmetric catalytic aziridinations has received the most attention [2]. A variety of methods have been developed for the synthesis of aziridines [9,12,13] including a ring closure reaction of 1,2-amino alcohols or their derivatives [14,15], ring opening of epoxides with metal azides [16,17], addition of α-haloester enolates to imines [18], transfer of a nitrene group to an alkene [19,20], and the reactions between diazo esters and imines mediate either by carbene transfer catalysts [21–23] or Lewis acid catalysts [24–29].

The aziridination catalysed by the transition metals, which is defined as a [2+1] cycloaddition between a carbene-type species and imines (Scheme 1), is an important synthetic method to obtain aziridine rings. Some transition metals such as rhodium and copper are found to be able to catalyse the aziridination [30,31].

As illustrated in Scheme 2, it is also generally accepted that copper-catalysed aziridination proceeds via a copper–carbene complex **E**, which is formatted by association of the diazo compound **D** and the active catalyst **B** with concomitant extrusion of nitrogen; and then the attack of imines **F** on the copper–carbene intermediate **E** leads to the asymmetric aziridine **G**. In copper-catalysed asymmetric aziridination, the copper–carbene intermediate plays an important role. The copper–carbene complex is better in stabilisation and enantioselectivity, compared with a free carbene, and has been detected as a reaction intermediate in the experiment [32].

Ikeno et al. [33] have studied some metal–carbene complexes such as Co-, Cu- and Ru-carbenes at B3LYP/6-31G(d) or B3LYP/LANL2DZ levels. The formation of copper–carbene intermediate has been studied by Salvatella and others [34] at the B3LYP/6-31G(d) level. Some copper–carbene complexes [35] and copper-catalysed asymmetric cyclopropanation [36] have been studied by us at B3LYP/6-31G(d) or B3LYP/6-31G levels. The theoretical data available for the reaction mechanism of the aziridination of diazoacetate with imines are rather limited. The detailed quantum chemical studies on the mechanism of the metal-catalysed aziridination are hardly reported. Therefore, in order to understand the mechanism of the metal-catalysed aziridination in detail, chiral bisoxazoline-copper(I)-catalysed asymmetric

*Corresponding author. Email: qingxim@sdau.edu.cn

ISSN 0892-7022 print/ISSN 1029-0435 online

DOI: 10.1080/08927020903096056
http://www.informaworld.com

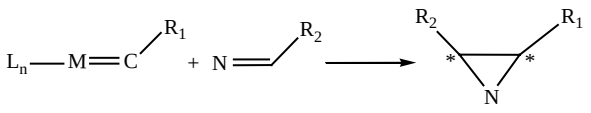

Scheme 1. Transition metals-catalysed aziridination of diazoacetate with imines.

aziridination of diazoacetate with imines is studied in the present work.

2. Model and computation

The present studies are based on chiral bisoxazoline–copper(I)-catalysed aziridination of diazoacetate with imines (Scheme 3) [30,31]. This aziridination is suggested as the following (illustrated in Schemes 4 and 5): the decomposition of the catalyst, the bisoxazoline–copper(I) complex, leading to oxazoline and the active oxazoline–copper(I) catalyst **CA2**; the reaction of diazoacetate with the active catalyst **CA2** generating the catalyst–diazoacetate complex **M1**; the decomposition of N_2 in **M1** leading to the copper(I)–carbene intermediate **M2**; the reaction of **M2** with imines resulting in the copper(I)–carbene–imine complexes **M3**; the formation of the catalyst–aziridine carboxylate complexes **M4** or **M5**; the decomposition of complexes **M4** or **M5** leading to the aziridine carboxylate and regenerating the active catalyst **CA2**. In the present model shown in Scheme 3, the methylene imines and diazo methyl acetate are substituted, respectively, for the imines and diazo ethyl acetate. As shown in Scheme 6, the methylene imines can attack on the *re*-surface or the *si*-surface of the copper(I)–carbene intermediate **M2**, which leads to four plausible reaction paths. In the following discussion, the attack of imines on the *re*-surface of **M2** is marked by 'a' and its attack on the *si*-surface is marked by 'b'. The numbers (1–7) marking the atoms are shown in Scheme 4.

All intermediates and transition states are fully optimised by means of the density functional theory (DFT), with Becke's three-parameter functional (B3) [37] and Lee, Yang and Parr (LYP) correlation energies [38,39], at the B3LYP/6-31G(d) level. The vibrational analysis and the natural bond orbital (NBO) analysis [40–48] of all the optimised structures are also performed at the B3LYP/6-31G(d) level. All the species are positively identified for local minima with zero of the number of imaginary frequencies and for transition states with the sole imaginary frequency. The transition states were verified by intrinsic reaction coordinate [49] calculations and by animating the negative eigenvector coordinates with a visualisation program (Molekel 4.3) [50,51]. The intermediates were characterised

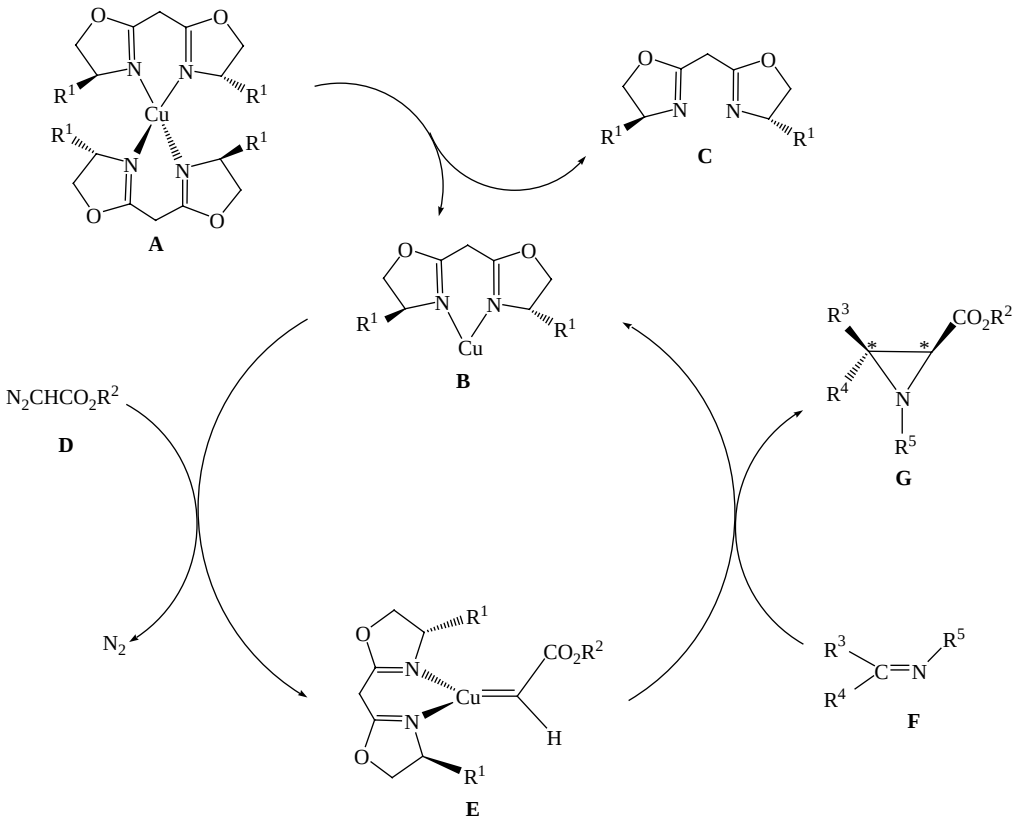

Scheme 2. Possible reaction mechanism of copper-catalysed aziridination of diazoacetate with imines.

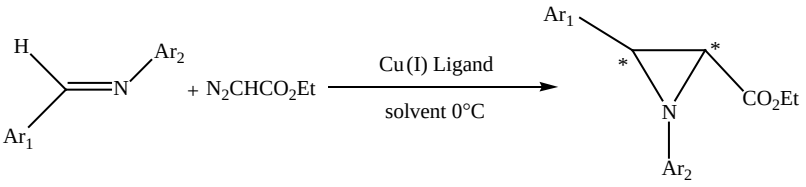

Scheme 3. Copper-catalysed asymmetric aziridination of diazoacetate with imines.

by all real frequencies, and transition states had the sole imaginary frequency (Table 1). All these computations are carried out using the Gaussian 03 program package [52]. Total Gibbs free energies rectified with zero-point energies (ZPE), G, formation Gibbs free energies, ΔG, reaction Gibbs free energy barriers, $\Delta G^{\neq}$, and the first two vibrational frequencies, ν_1 and ν_2, are summarised in Table 1.

The topological properties of the electronic charge density have been characterised using the atoms in molecules (AIM) [53] method of Bader with the AIM 2000 program package [54].

3. Results and discussion

3.1 Catalyst

The optimised structure of the catalyst, chiral bisoxazoline–copper(I) **CA**, is illustrated in Figure 1. It is a C_2-symmetry complex and its lowest vibrational frequency

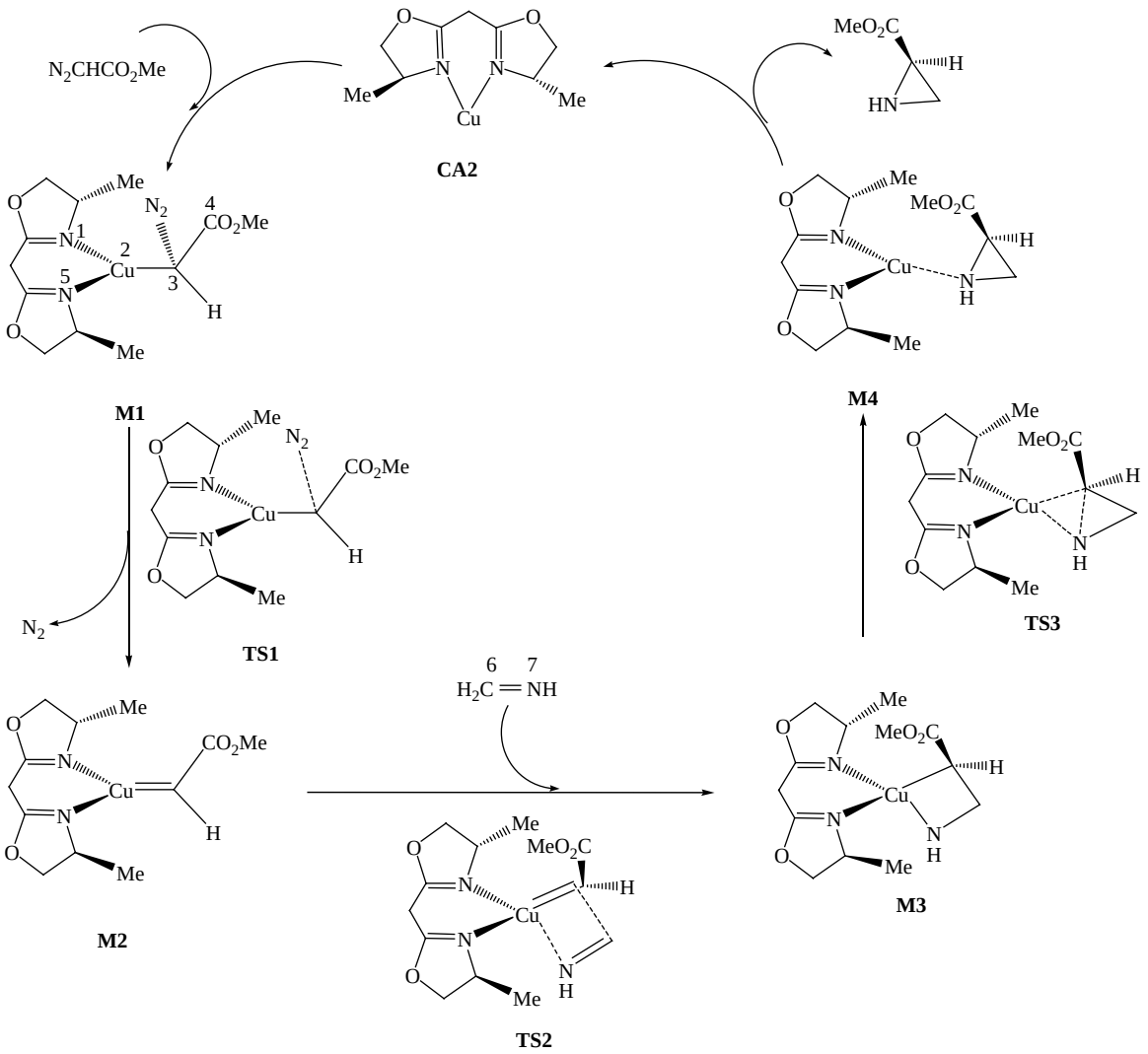

Scheme 4. Proposed mechanism of copper(I)-catalysed aziridination: reaction mode I.

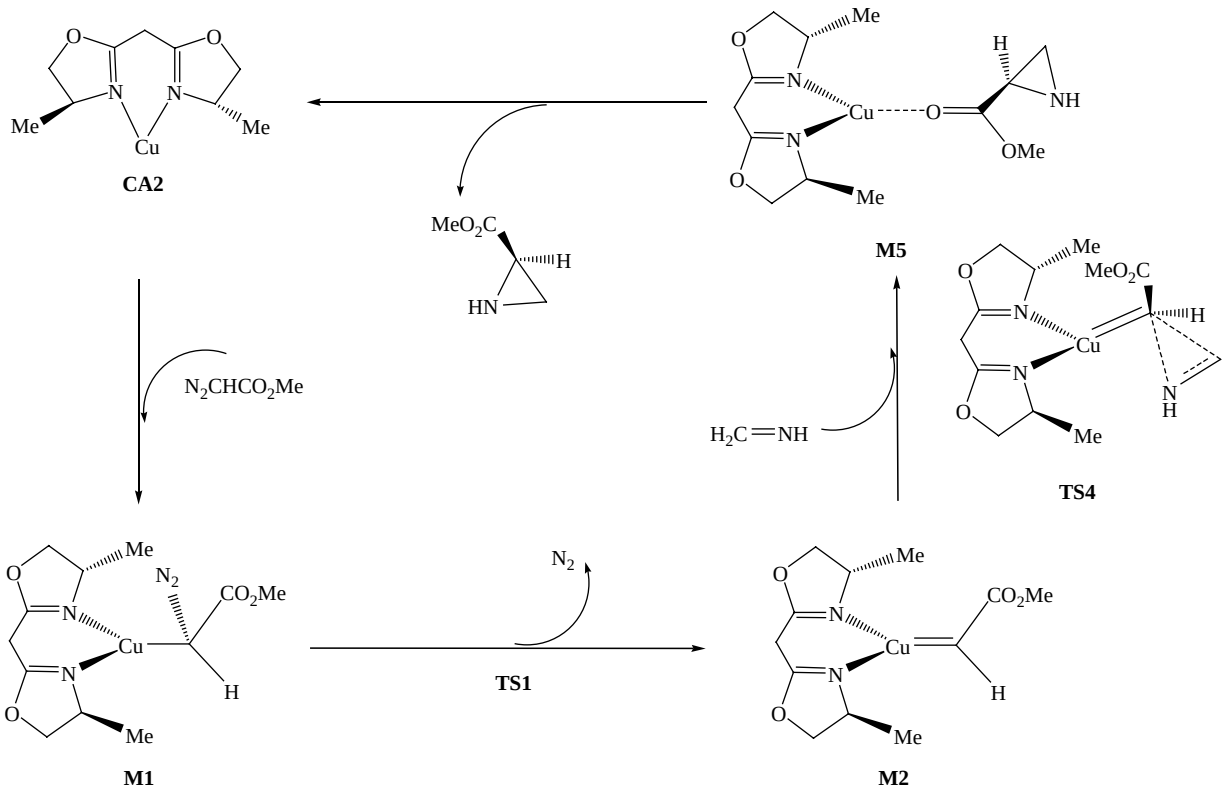

Scheme 5. Proposed mechanism of copper(I)-catalysed aziridination: reaction mode II.

is positive. There is a Cu—N—C—C—C—N six-membered ring in the catalyst **CA** and the six atoms are nearly in the same plane (as shown, most of the intermediates and transition states have this character). The Cu—N and C—N bonds are 2.008 and 1.283 Å, respectively. And thus Cu—N and C—N bonds are 1.841 and 1.295 Å in the active catalyst **CA2** (Figure 2).

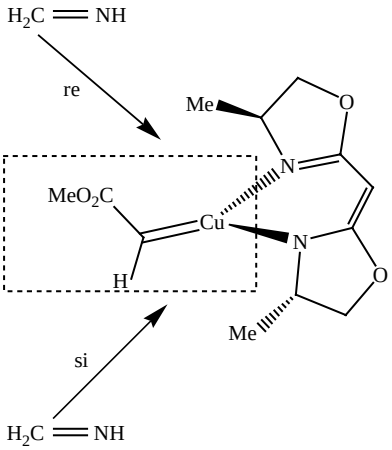

Scheme 6. Attack of imines on copper–carbene intermediate **M2**.

3.2 Formation of copper(I)–carbene intermediate

As illustrated in Scheme 4 and Figure S2, the reaction of diazoacetate (**R1**) with the active catalyst **CA2** leads to the catalyst–diazoacetate complex **M1**, and then the decomposition of N_2 in the complex **M1** generates the copper(I)–carbene intermediate **M2** via the transition state **TS1**.

Figure 3 shows that, in the catalyst–diazoacetate complexes **M1a** and **M1b**, the Cu(2)—C(3) and C(3)—N(N_2) bonds are **M1a**: 1.981, 1.355 Å and **M1b**: 1.951, 1.374 Å, respectively. Compared with those of diazoacetate, C(3)—N(N_2) bonds become longer by about 0.06 Å, which possibly resulted from the formation of Cu(2)—C(3) bonds. As illustrated in NBO analysis, Cu(2)—C(3) bond is composed of 8% s orbital of copper and 92% p orbital of carbon, and the orbital energies are **M1a**: −1180.74 and **M1b**: −1278.28 kJ/mol. The N(1)—Cu(2)—C(3)—C(4) and N(1)—Cu(2)—C(3)—N(N_2) torsion angles are, respectively, 87.4, −161.0 for **M1a** and 140.2°, 15.6° for **M1b**. In the transition states **TS1a** and **TS1b**, C(3)—N(N_2) bonds are stretched considerably and Cu(2)—C(3) bonds are shortened compared with those in the complexes **M1** (**M1** → **TS1**, C(3)—N(N_2) bond: 1.4 → 1.8 Å, Wiberg bond order P_{ij}: 0.98 → 0.48, the electron densities ρ of the bond critical points (BCPs): 0.26 → 0.10 e/Å^3; Cu(2)—C(3) bond: 2.0 → 1.8 Å, P_{ij}:

Table 1. Total Gibbs free energies, G (× 2625.5 kJ/mol), formation Gibbs free energies, ΔG (kJ/mol), reaction Gibbs free energy barriers, $\Delta G^{\neq}$(kJ/mol), and frequencies (cm^{-1}) for all the compounds.

	ZPE	G	ΔG	$\Delta G^{\neq}$	ν_1	ν_2
CA2	0.2324	−2251.2619			17.09	27.94
R1	0.0770	−376.5791			99.41	132.36
R2	0.0401	−94.6091			1084.08	1091.42
M1a	0.3108	−2627.8696	−75.09		19.82	23.45
M1b	0.3111	−2627.8691	−73.78		11.61	23.69
TS1a	0.3088	−2627.8562		35.18	385.04i	18.85
TS1b	0.3089	−2627.8570		31.77	395.46i	17.60
N_2	0.0056	−109.5370			2457.66	
M2	0.3012	−2518.3595	−70.57		20.17	30.22
			−71.89			
TS2a1	0.3439	−2612.9390		77.71	316.10i	20.26
TS2a2	0.3443	−2612.9505		47.52	239.06i	24.58
TS2b1	0.3445	−2612.9439		64.85	284.36i	25.55
TS2b2	0.3443	−2612.9448		62.49	238.34i	30.26
M3a1	0.3486	−2613.0041	−93.20		22.72	28.26
M3a2	0.3488	−2613.0091	−106.33		17.61	25.87
M3b1	0.3488	−2612.9987	−79.03		26.34	30.89
M3b2	0.3490	−2613.0041	−93.21		8.40	25.91
TS3a1	0.3469	−2612.9957		22.05	255.36i	25.30
TS3a2	0.3470	−2612.9992		25.99	299.65i	17.02
TS3b1	0.3473	−2612.9923		16.80	155.66i	22.84
TS3b2	0.3473	−2612.9930		29.14	293.65i	15.61
M4a1	0.3485	−2613.0291	−65.64		18.68	20.50
M4a2	0.3489	−2613.0249	−41.48		14.18	18.69
M4b1	0.3484	−2613.0289	−79.29		13.45	17.26
M4b2	0.3485	−2613.0219	−46.73		9.66	14.37
P1(*R*)	0.1141	−361.7127			69.83	127.91
P2(*S*)	0.1140	−361.7127			69.90	128.02
TS4a	0.3444	−2612.9342		90.32	261.9i	23.5
TS4b	0.3443	−2612.9348		88.74	256.0i	14.6
M5a	0.3474	−2613.0124	−115.00		12.28	17.27
M5b	0.3474	−2613.0126	−115.52		10.19	16.48

0.25 → 0.38, ρ: 0.10 → 0.14; Table S1). NBO analysis shows that Cu(2)—C(3) bond is composed of 10% s orbital of copper and 90% sp^2 hybrid orbital of carbon, and the orbital energies are −1493.67 and −1485.72 kJ/mol, respectively, and so there is a σ bond between copper and carbon which is different from **M1**. As shown in Figure 4,

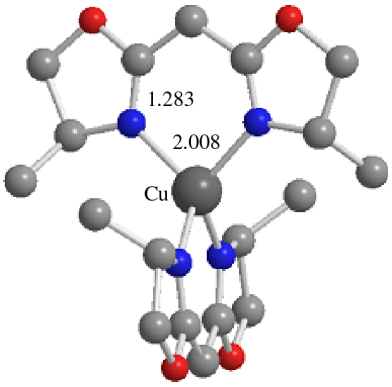

Figure 1. Optimised structure of bisoxazoline–copper(I) **CA** (bond distances in Å, all hydrogens were omitted).

the copper–carbene intermediate **M2** has only one geometry, and the N(1)—Cu(2)—C(3)—H and N(1)—Cu(2)—C(3)—C(4) torsion angles are 90.0° and 100.8°, respectively. In **M2**, Cu(2)—C(3) bond is 1.782 Å, which is shorter than **M1**. As illustrated in NBO analysis, Cu(2)—C(3) bond shows strong single-bonded character, and the natural bond orbital energy is −1102.16 kJ/mol. And thus, NBO analysis also shows that the Cu(2)—C(3) bond has some double-bonded character, and the bond order is >1 and ≈1.1. The NBO charges of copper and carbon atoms of Cu(2)—C(3) bond are 1.174 and −0.602.

3.3 Reaction mode I: the direct attack of imines on Cu—C bond of copper(I)–carbene intermediate

As illustrated in Scheme 4, the reaction of **M2** with imines leads to the copper–carbene–imine complexes **M3**, and the responding transition state is **TS2**. The elimination of the copper–carbene–imine complexes **M3** leads, via the transition states **TS3**, to the catalyst–aziridine carboxylate complexes **M4**; the decomposition of **M4** results in the aziridine carboxylate and regenerates the active catalyst **CA2**.

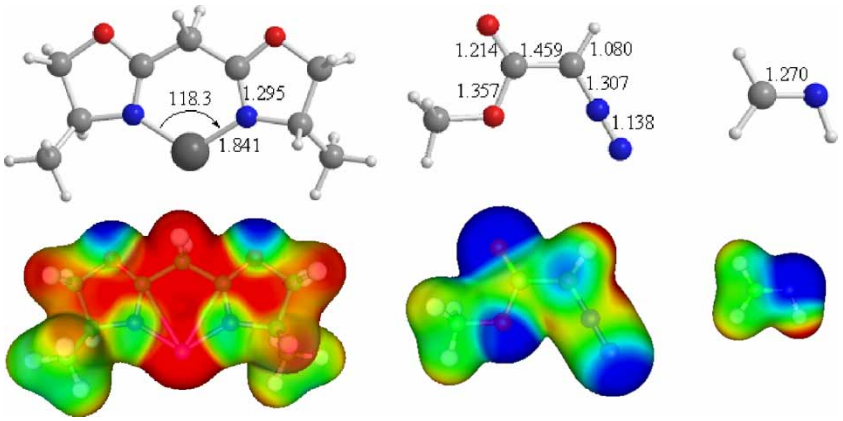

CA2 (μ = 0.234) **R1** (μ = 0.956) **R2** (μ = 1.973)

Figure 2. Optimised structures and electrostatic pictures of **CA2**, **R1** and **R2** (bond distances in Å, angles in degree, moment dipoles, μ, in Debye).

Scheme 6 shows that the attack of imines on **M2** has two reaction modes: from the *re*-surface or the *si*-surface of **M2**.

3.3.1 Formation of copper(I)–carbene–imine complex

The transition states **TS2a1**, **TS2a2**, **TS2b1** and **TS2b2** have sole imaginary frequencies, in correspondence with the stretching vibrations of the Cu(2)—N(7) and C(3)—C(6) bonds. The Cu(2)—N(7) and C(3)—C(6) distances are about 2.4 and 1.4 Å, respectively. Obviously, the Cu(2)—N(7) and C(3)—C(6) bonds are strengthened markedly. It is shown by these results that the Cu(2)—N(7) and C(3)—C(6) bonds could be formatted at the same time. Compared with those in imines and **M2**, the C(6)—N(7) and Cu(2)—C(3) bonds are weakened and lengthened by about 0.05 and 0.12 Å, which results from the formation of the Cu(2)—N(7) and C(3)—C(6) bonds. As demonstrated in Figure 5, the transition states involve a Cu(2)—C(3)—C(6)–N(7) four-membered ring, and the electron densities ρ of the ring critical points (RCPs) are about 0.03. In the copper–carbene–imine complexes **M3**, the C(6)—N(7) bonds are about 1.5 Å. Furthermore NBO analysis shows that the C(6)—N(7) bond displays strong single-bonded character, and the natural bond orbital energy of the σ bond is about −1300 kJ/mol, which is higher than those in imines (−2300 kJ/mol). The four atoms Cu(2), C(3), C(6) and N(7) are nearly coplanar and there is a RCP, with about 0.06 of electron density, inside the area encircled by the four atoms. There is a little angle between the Cu(2)—C(3)—C(6)—N(7) four-membered ring and the N(1)—Cu(2)—N(5) plane.

As discussed above, in the reaction channels **M2** → **TS2** → **M3**, the Cu(2)—N(7) and C(3)—C(6) bonds are decreased (Cu(2)—N(7) bond: ∞ → 2.4 → 1.9 Å; C(3)—C(6) bond: ∞ → 1.9 → 1.5 Å). These results are also demonstrated by analysing the changes of Wiberg bond orders and the electron densities of the BCPs (Table S2, Cu(2)—N(7) bond, P_{ij}: 0.00 → 0.23 → 0.27, ρ: 0.00 → 0.12 → 0.14; C(3)—C(6) bond, P_{ij}: 0.00 → 0.16 → 0.82, ρ: 0.00 → 0.03 → 0.25). These also confirm that the Cu(2)—N(7) and C(3)—C(6) bonds could be formatted at the same time.

In addition, we tried to compute another four transition states, **TS2**: when imines attack on **M2** leading to **M3**, N(7) attacks on the carbene carbon, and thus C(6) attacks on copper. But all of our efforts failed.

3.3.2 The elimination: formation of copper(I)–aziridine carboxylate complex

The transition states **TS3a1**, **TS3a2**, **TS3b1** and **TS3b2** have sole imaginary frequencies which are in correspondence with the stretching vibrations of the Cu(2)—C(3) and Cu(2)—N(7) bonds. The Cu(2)—C(3), Cu(2)—N(7) and C(3)—N(7) bonds are about 2.2, 1.9 and 1.8 Å, respectively. Compared with **M3**, the Cu(2)—C(3) and Cu(2)—N(7) bonds are stretched, the C(3)—N(7) bonds are shortened. As demonstrated in Figure S4, the transition states involve a Cu(2)—C(3)—C(6)—N(7) four-membered ring, and the electron densities ρ of the RCPs are about 0.07. In the complexes **M4a1** and **M4b1**, there is a Cu(2)—N(7)—C(3)—C(4)—O(O═C) five-membered ring, and the Cu(2)—N(7) and Cu(2)—O(O═C) bonds are 2.0 and 2.3 Å, respectively. But in the complexes **M4a2** and **M4b2** the same five-membered ring was not found. Only the Cu(2)—N(7) bond is formatted, and the bond is 1.9 Å. So the coordination number of **M4a1** and **M4b1** is four, but that of **M4a2** and **M4b2** is three.

As discussed above, in the reaction channels **M3** → **TS3** → **M4**, the Cu(2)—C(3) and Cu(2)—N(7) bonds are stretched, and the C(3)—N(7) bond is shortened (e.g. C(3)—N(7) bond: 2.2 → 1.9 → 1.5 Å). These results

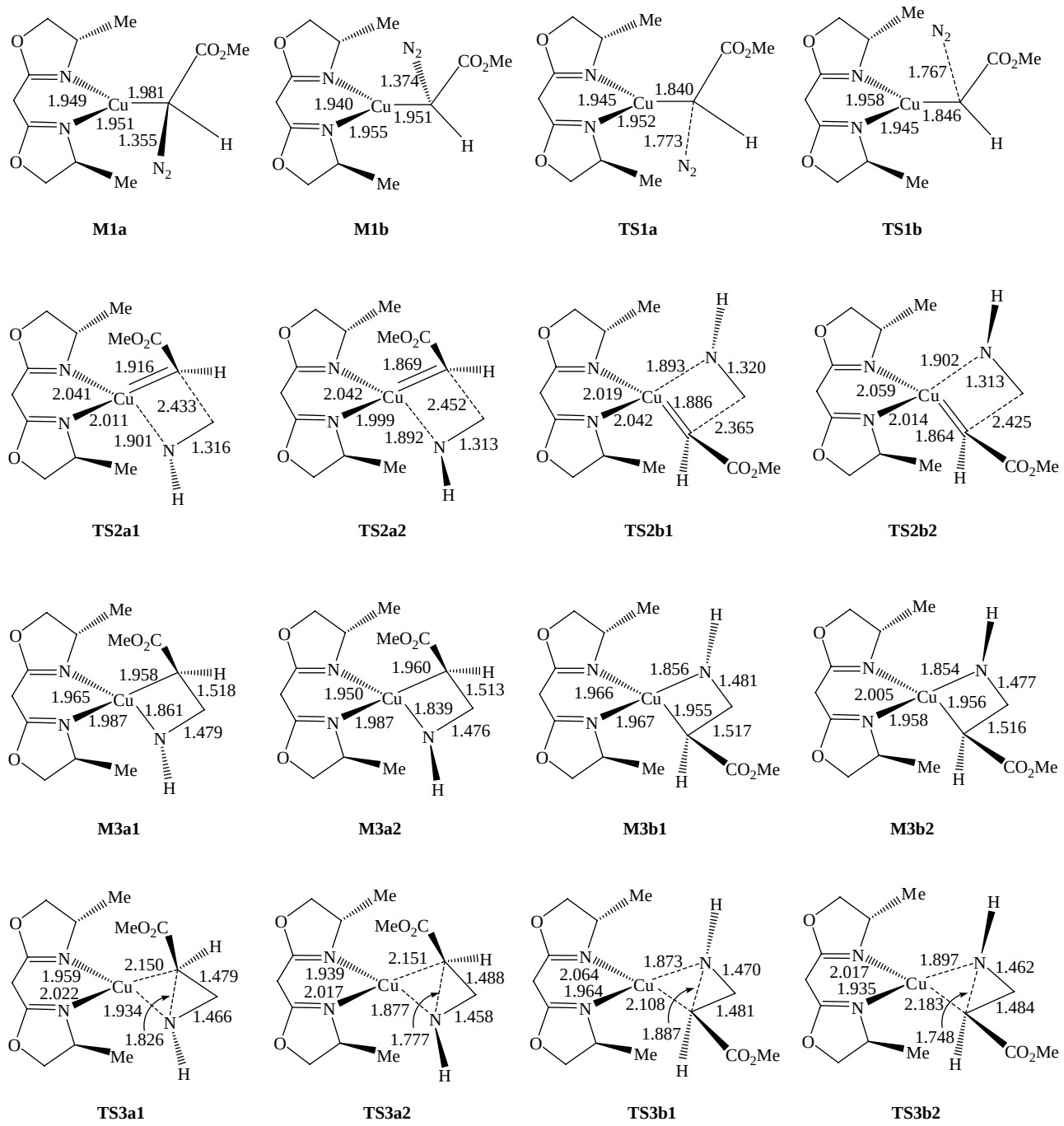

Figure 3. Optimised structures for intermediates and transition states of copper-catalysed asymmetric aziridination (bond distances in Å).

are also demonstrated by analysing the changes of Wiberg bond orders and the electron densities of the BCPs (Tables S2 and S3, e.g. C(3)—N(7) bond, P_{ij}: 0.00 → 0.45 → 0.70, ρ: 0.00 → 0.00 → 0.25). It is shown by the present computations that the fractures of the Cu(2)—C(3) and Cu(2)—N(7) bonds and the formation of the C(3)—N(7) bond may occur at the same time.

3.4 Reaction mode II: the direct attack of imines on carbene–carbon of copper(I)–carbene intermediate

As illustrated in Scheme 5 and Figure S5, the double bonds $\pi_{C(6)—N(7)}$ of imines attack directly on the carbene–carbon of copper(I)–carbene intermediate **M2**, leading to the catalyst–aziridine carboxylate complexes **M5**, and the responding transition states **TS4**. The decomposition

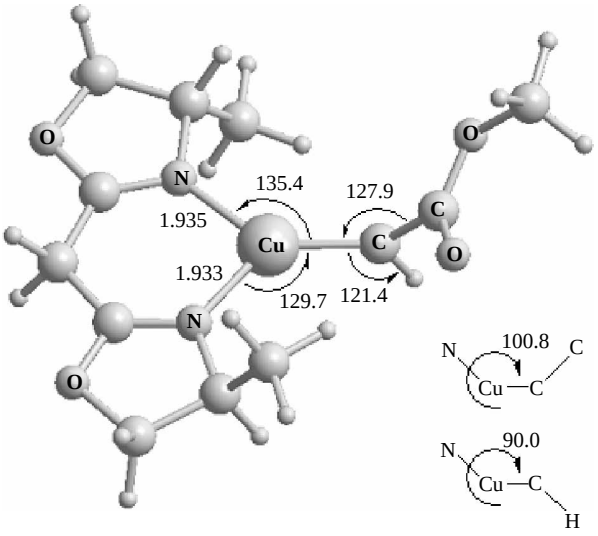

Figure 4. Optimised structure of copper–carbene intermediate **M2** (bond distances in Å, angles and torsion angles in degree).

of **M5** results in the aziridine carboxylate and regenerates the active catalyst **CA2**.

Figure 6 shows that C(3)—C(6) and C(3)—N(7) bonds of **TS4a** and **TS4b** are 2.1 and 2.3 Å, respectively. Clearly, there is significant interaction between C(3) and C(6) and N(7), which is demonstrated by analysing the changes of Wiberg bond orders and the electron densities of the BCPs (Table S4, e.g. C(3)—C(6) bond, P_{ij}, **M2**: 0.00 → **TS4**: 0.29 → **M5**: 0.75, ρ, **M2**: 0.00 → **TS4**: 0.06 → **M5**: 0.24). It is shown by these results that the C(3)—C(6) and C(3)—N(7) bonds may be formatted at the same time. The formation of C(3)—C(6) and C(3)—N(7) bonds makes the Cu(2)—C(3) and $\pi_{C(6)-N(7)}$ bonds fractured.

3.5 Stabilisation interaction energies

The second-order perturbation stabilisation energies $E(2)$ obtained by NBO analysis are summarised in Table S5. It can be used to describe the delocalisation trend of electrons from the donor bond to the acceptor bond. In NBO analysis, if the stabilisation interaction energy $E(2)$ between a donor bonding orbital and an acceptor

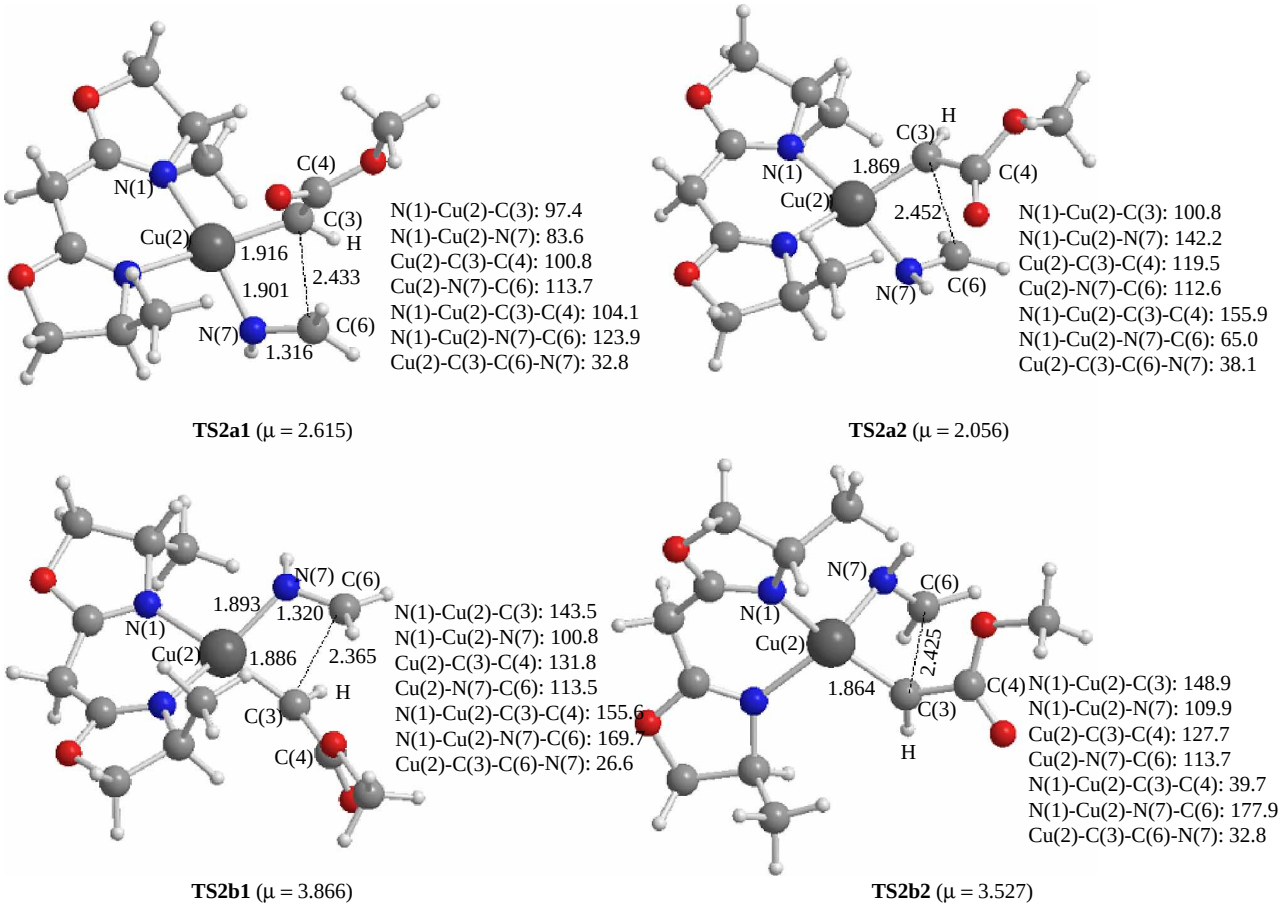

Figure 5. Optimised structures of **TS2** (bond distances in Å, angles and dihedral angles in degree, moment dipoles, μ, in Debye).

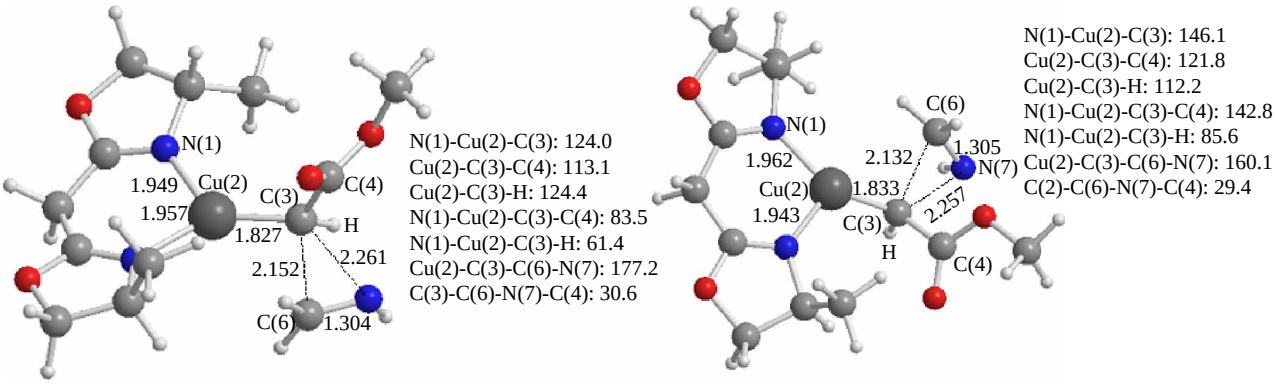

TS4a (μ = 4.082) **TS4b** (μ = 4.364)

Figure 6. Optimised structures of **TS4** (bond distances in Å, angles and dihedral angles in degree, moment dipoles, μ, in Debye).

bonding orbital is large, there is a strong interaction between the two bonds.

As demonstrated in Table S5, in **M1** and **TS1**, there is a strong donor–acceptor interaction between the lone pair orbital of the atoms N(1) and N(5) and the σ* antibond orbital of the Cu(2)—C(3) bond. These confirm that the electrons in the lone pair orbitals of N(1) and N(5) are easy to transfer to the σ* antibond orbital of Cu(2)—C(3) bond, which makes **M1** and **TS1** to be of better stability. In the transition states **TS2**, there is a strong interaction between the π orbital of the C(6)—N(7) bond and the σ* antibond orbital of Cu(2)—C(3) bond, which makes the electrons in the π orbital transfer easily to the σ* antibond orbital of Cu(2)—C(3) bond, so the π orbital of the C(6)—N(7) bond has a tendency to fracture. In the transition states **TS3**, the electrons in the σ orbital of C(3)—N(7) bond are easy to transfer to the LP*(6) orbital of copper, and the electrons in the LP(5) orbital of copper are easy to transfer to the σ* orbital of C(3)—N(7) bond, which makes **TS3** more stable. In **TS4**, the electrons in the π orbital of Cu(2)—C(3) bond are easy to transfer to the π* antibond orbital of C(6)—N(7) bond; and the electrons in the π orbital of C(6)—N(7) bond are easy to transfer to the σ* antibond orbital of Cu(2)—C(3) bond, which makes **TS4** more stable and redounds to the formation of C(3)—C(6) and C(3)—N(7) bonds.

3.6 Copper(I)-catalysed aziridination

As discussed above, chiral bisoxazoline–copper(I)-catalysed aziridination of diazoacetate with imines has two reaction modes: I and II. As shown in Scheme 4, in reaction mode I, the aziridination goes mainly through the catalyst–diazoacetate complex **M1**, the copper(I)–carbene intermediate **M2**, the copper–carbene–imine complex **M3** and the catalyst–aziridine carboxylate complex **M4**, and the responding transition states are **TS1**, **TS2** and **TS3**. In reaction mode II (Scheme 5), the aziridination goes through the catalyst–diazoacetate complex **M1**, the copper(I)–carbene intermediate **M2**, and the catalyst–aziridine carboxylate complex **M5**, and the responding transition states are **TS1** and **TS4**.

Table 1 shows that the formation of the complexes **M1**, **M2**, **M3**, **M4** and **M5** are exothermic, and the released Gibbs free energies are −75, −70, −90, −60 and −115 kJ/mol, respectively. In addition, the copper(I)-catalysed asymmetric aziridination is exothermic, and the total released Gibbs free energy is about −170 kJ/mol.

The transition states **TS1a** and **TS1b** are related to the fracture of C(3)—N(N_2) bond, and their reaction Gibbs free energy barriers are 35.18 and 31.77 kJ/mol, respectively. The transition states **TS2** have strained Cu(2)—C(3)—C(6)—N(7) four-membered rings, being related to the formation of the Cu(2)—N(7) and C(3)—C(6) bonds, and their reaction Gibbs free energy barriers are about 60 kJ/mol. The transition states **TS3** also have a Cu(2)—C(3)—C(6)—N(7) four-membered ring, being related to the fractures of the Cu(2)—C(3) and Cu(2)—N(7) bonds and the formation of the C(3)—N(7) bond, and their reaction Gibbs free energy barriers are about 25 kJ/mol. **TS4** are the transition states of the direct attack of imines on carbene–carbon of copper(I)–carbene intermediate, being related to the formation of the C(3)—C(6) and C(3)—N(7) bonds, and their reaction Gibbs free energy barriers are about 90 kJ/mol. Obviously, in reaction mode I, the reaction Gibbs free energy barriers of **TS2** are higher than those of **TS1** and **TS3**, so the formation of the copper(I)–carbene–imine complex **M3** (i.e. the attack of imines on copper–carbon(carbene) of copper–carbene intermediate **M2**) is the rate-determining step. In reaction mode II, the reaction Gibbs free energy barriers of **TS4** are higher than those of **TS1**, so the formation of the catalyst–aziridine carboxylate complex **M5** (i.e. the direct attack of imines on carbene–carbon of copper(I)–carbene intermediate **M2**) is the rate-determining step. Because the reaction Gibbs free energy

barriers of **TS2** are lower than those of **TS4**, the reaction mode I is dominant for the copper-catalysed aziridination of diazoacetate with imines.

In reaction mode I, the atoms C(3) of the copper–carbene intermediate **M2** are prochiral. As shown in Figure 3, in **M3**, **M4**, **TS2** and **TS3**, the atoms C(3) are asymmetric, so these reaction channels can lead to two asymmetric products. Therefore, the formation of the copper(I)–carbene–imine complex **M3** is the chirality-limiting step for the copper-catalysed asymmetric aziridination of diazoacetate with imines. As summarised in Table 1, the reaction Gibbs free energy barriers of the transition states **TS2a1**, **TS2a2**, **TS2b1** and **TS2b2** are 77.71, 47.52, 64.85 and 62.49 kJ/mol, respectively. It is clear that the reaction channel **CA2 → M1a → TS1a → M2 → TS2a2 → M3a2 → TS3a2 → M4a2 → P1**(*R*) is the most favourable one. The dominant products obtained from this reaction channel are of (*R*)-chirality.

4. Conclusion

In this study, we have investigated chiral bisoxazoline–copper(I)-catalysed asymmetric aziridination of diazoacetate with imines using the DFT. All the intermediates and the transition states were optimised completely at the B3LYP/6-31G(d) level. Calculation results confirm that copper-catalysed asymmetric aziridination of diazoacetate with imines is exothermic, and the total released Gibbs free energy is about − 170 kJ/mol. The copper(I)-catalysed aziridination has two reaction modes: I and II, and thus the reaction mode I is dominant. The formation of the copper(I)–carbene–imine complex **M3** (i.e. the attack of imines on copper–carbon(carbene) of copper–carbene intermediate **M2**) is the rate-determining step and the chirality-limiting step for the copper-catalysed asymmetric aziridination. The reaction channel **CA2 → M1a → TS1a → M2 → TS2a2 → M3a2 → TS3a2 → M4a2 → P1**(*R*) is the most favourable one. The dominant products predicted theoretically are of (*R*)-chirality.

References

[1] D. Tanner, *Stereocontrolled synthesis via chiral aziridines*, Pure. Appl. Chem. 65 (1993), pp. 1319–1328.

[2] D. Tanner, *Chiral aziridines – their synthesis and use in stereoselective transformations*, Angew. Chem. Int. Ed. Engl. 33 (1994), pp. 599–619.

[3] W. McCoull and F.A. Davis, *Recent synthetic applications of chiral aziridines*, Synthesis. (2000), pp. 1347–1365.

[4] L. Dubois and R.H. Dodd, *Stereocontrolled synthesis of aziridine-2-lactones from D-ribose and D-lyxose*, Tetrahedron. 49 (1993), pp. 901–910.

[5] D. Tanner, C. Birgersson, and H.K. Dhaliwal, *Nucleophilic ring opening of C_2–symmetric aziridines. Synthetic equivalents for the β-cation of aspartic acid*, Tetrahedron Lett. 31 (1990), pp. 1903–1906.

[6] M.E. Piotti and H. Alper, *Inversion of stereochemistry in the $Co_2(CO)_s$–catalyzed carbonylation of aziridines to β-lactams. The first synthesis of highly strained* trans*-bicyclic β-lactams*, J. Am. Chem. Soc. 118 (1996), pp. 111–116.

[7] K. Tsuboyama, S. Tsuboyama, and M. Yanagita, *Stereoregularity of poly-(R)-2-ethylaziridine*, Bull. Chem. Soc. Jpn. 40 (1967), pp. 2954–2957.

[8] C. Gaebert and M. Mattay, [3+2] *Cycloadditions and nucleophilic additions of aziridines under C—C and C—N bond cleavage*, Tetrahedron, 53 (1997), pp. 14297–14316.

[9] H.M.I. Osborn and J. Sweeney, *The asymmetric synthesis of aziridines*, Tetrahedron: Asymm. 8 (1997), pp. 1693–1715.

[10] A. Padwa, A.D. Woolhouse, A.R. Katritzky, C.W. Rees and W. Lwowski, (eds), *Comprehensive Heterocyclic Chemistry*, Vol. 7, Pergamon, Oxford, 1984, p. 47.

[11] O.C. Dermer and G.E. Ham, *Ethylenimine and Other Aziridines*, Academic Press, New York, 1969.

[12] E.N. Jacobsen, in *Comprehensive Asymmetric Catalysis*, E. N. Jacobsen, A. Pfaltz and H. Yamamoto, eds.,Vol. 2, Springer-Verlag, Berlin/Heidelberg/New York, 1999, p. 607.

[13] R.S. Atkinson, *3-Acetoxyaminoquinazolinones (QNHOAc) as aziridinating agents: ring-opening of N-(Q)-substituted aziridines*, Tetrahedron. 55 (1999), pp. 1519–1559.

[14] J.W. Kelly, N.L. Eskew, and S.A. Evans, *Cyclodehydration of N- and C-substitnted .beta.-amino alcohols to the corresponding aziridines with diethoxytriphenylphosphorane*, J. Org. Chem. 51 (1986), pp. 95–97.

[15] E. Kuyl-Yeheskiely, G.A. Lodder, G.A. van der Marel, and J.H. van Boom, *One-step synthesis of optically active benzyl N-trityl-L-aziridine-2-carboxylic esters*, Tetrahedron Lett. 33 (1992), pp. 3013–3016.

[16] J. Legters, L. Thijs, and B. Zwanenburg, *A convenient synthesis of optically active lH-aziridine-2-carboxylic acids (esters)*, Tetrahedron Lett. 30 (1989), pp. 4881–4884.

[17] D. Tanner and P. Somfai, *An aziridine route to chiral fl-lactams a novel entry to (+)-thienamycin*, Tetrahedron Lett. 28 (1987), pp. 1211–1214.

[18] G. Cainelli, M. Panunzio, and D. Giacomoni, *Studies on N-metallo imines: synthesis of N-unsubstituted aziridines from N-trimethylsilyl imine and lithium etiolates of α-halo esters*, Tetrahedron Lett. 31 (1991), pp. 121–124.

[19] D.A. Evans, M.M. Faul, M.T. Bilodeau, B.A. Anderson, and D.M. Barnes, *Bis(oxazoline)-copper complexes as chiral catalysts for the enantioselective aziridination of olefins*, J. Am. Chem. Soc. 115 (1993), pp. 5328–5329.

[20] J.A. Halfen, J.K. Hallman, J.A. Schultz, and J.P. Emerson, *Remarkably efficient olefin aziridination mediated by a new copper(II) complex*, Organometallics 18 (1999), pp. 5435–5437.

[21] K.B. Hansen, N.S. Finney, and E.N. Jacobsen, *Carbenoid transfer to imines: a new asymmetric catalytic synthesis of aziridines*, Angew. Chem. Int. Ed. Engl. 34 (1995), pp. 676–678.

[22] K.G. Rasmussen and K.A. Jørgensen, *Catalytic formation of aziridines from imines and diazoacetate*, J. Chem. Soc. Chem. Commun. (1995), pp. 1401–1402.

[23] T.B. Gunnoe, P.S. White, J.L. Templeton, and L. Casarrubios, *Electrophilic tungsten(II) methylene carbene complexes: adduct formation, methylene transfer, and catalysis of aziridine formation from imines and ethyl diazoacetate*, J. Am. Chem. Soc. 119 (1997), pp. 3171–3172.

[24] H.-J. Ha, K.-H. Kang, J.-M. Suh, and Y.-G. Ahn, *A new synthesis of aziridine-2-carboxylates by reaction of hexahydro-1,3,5-triazines with alkyldiazoacetates in the presence of tin(IV) chloride*, Tetrahedron Lett. 37 (1996), pp. 7069–7070.

[25] L. Casarrubios, J.A. Perez, M. Brookhart, and J.L. Templeton, *Lewis acid-catalyzed synthesis of aziridines*, J. Org. Chem. 61 (1996), pp. 8358–8359.

[26] K.G. Rasmussen and K.A. Jørgensen, *Metal-catalysed reactions of imines with ethyl diazoacetate leading to aziridines*, J. Chem. Soc. Perkin Trans. 1 (1997), pp. 1287–1291.

[27] W. Xie, J. Fang, J. Li, and P.G. Wang, *Aziridine synthesis in protic media by using lanthanide triflates as catalysts*, Tetrahedron. 55 (1999), pp. 12929–12938.

[28] J.C. Antilla and W.D. Wulff, *Catalytic asymmetric aziridination with a chiral VAPOL-boron Lewis acid*, J. Am. Chem. Soc. 121 (1999), pp. 5099–5100.

[29] K. Juhl, R.G. Hazell, and K.A. Jørgensen, *Catalytic enantioselective formation of aziridines from α-imino esters*, J. Chem. Soc. Perkin Trans. 1 (1999), pp. 2293–2297.
[30] A.-H. Li, L.-X. Dai, and V.K. Aggarwal, *Asymmetric ylide Reactions: epoxidation, cyclopropanation, aziridination, olefination, and rearrangement*, Chem. Rev. 97 (1997), pp. 2341–2372.
[31] S.-H. Lee, T.-D. Han, K. Yu, and K.-H. Ahn, *Aziridination of imines mediated by copper catalysts*, Bull. Korean. Chem. Soc. 22 (2001), pp. 449–450.
[32] B.F. Straub and P. Hofmann, *Copper(I) carbenes: the synthesis of active intermediates in copper-catalyzed cyclopropanation*, Angew. Chem. Int. Ed. Engl. 40 (2001), pp. 1288–1290.
[33] T. Ikeno, I. Iwakura, and T. Yamada, *Cobalt-carbene complex with single-bond character: intermediate for the cobalt complex-catalyzed cyclopropanation*, J. Am. Chem. Soc. 124 (2002), pp. 15152–15153.
[34] J.M. Fraile, J.I. García, V. Martínez-Merino, J.A. Mayoral, and L. Salvatella, *Theoretical (DFT) insights into the mechanism of copper-catalyzed cyclopropanation reactions. Implications for enantioselective catalysis*, J. Am. Chem. Soc. 123 (2001), pp. 7616–7625.
[35] Q. Meng and M. Li, *Theoretical insights of copper(I) carbenes*, J. Mol. Struct. (Theochem) 765 (2006), pp. 13–20.
[36] Q. Meng, M. Li, D. Tang, W. Shen, and J. Zhang, *Density functional studies on copper-catalyzed asymmetric cyclopropanation of diazoacetate with alkene*, J. Mol. Struct. (Theochem) 711 (2004), pp. 193–199.
[37] A.D. Becke, *Density-functional thermochemistry. III. The role of exact exchange*, J. Chem. Phys. 98 (1993), pp. 5648–5652.
[38] C. Lee, W. Yang, and R.G. Parr, *Development of the Colle-Salvetti correlation-energy formula into a functional of the electron density*, Phys. Rev. B 37 (1998), pp. 785–789.
[39] B. Miehlich, A. Savin, H. Stoll, and H. Preuss, Results *obtained with the correlation energy density functionals of Becke and Lee, Yang and Parr*, Chem. Phys. Lett. 157 (1989), pp. 200–206.
[40] E.D. Glendening, A.E. Reed, J.E. Carpenter and F. Weinhold, *NBO Version 3.1*.
[41] J.E. Carpenter and F. Weinhold, *Analysis of the geometry of the hydroxymethyl radical by the "different hybrids for different spins" natural bond orbital procedure*, J. Mol. Struct. (Theochem) 169 (1988), pp. 41–62.
[42] J.E. Carpenter, PhD thesis, University of Wisconsin, Madison, WI, (1987).
[43] J.P. Foster and F. Weinhold, *Natural hybrid orbitals*, J. Am. Chem. Soc. 102 (1980), pp. 7211–7218.
[44] A.E. Reed and F. Weinhold, *Natural bond orbital analysis of near-Hartree–Fock water dimmer*, J. Chem. Phys. 78 (1983), pp. 4066–4073.
[45] A.E. Reed and F. Weinhold, *Vibrational-rotational energy transfer in collisions of HF (v=4, J=20) with rare gases*, J. Chem. Phys. 83 (1985), pp. 1736–1740.
[46] A.E. Reed, R.B. Weinstock, and F. Weinhold, *Natural population analysis*, J. Chem. Phys. 83 (1985), pp. 735–746.
[47] A.E. Reed, L.A. Curtiss, and F. Weinhold, *Intermolecular interactions from a natural bond orbital, donor-acceptor viewpoint*, Chem. Rev. 88 (1988), pp. 899–926.
[48] F. Weinhold and J.E. Carpenter, *The structure of small molecules and ions*, Plenum. (1988), pp. 227–236.
[49] C. Gonzalez and H.B. Schlegel, *Reaction path following in mass-weighted internal coordinates*, J. Phys. Chem. 94 (1990), pp. 5523–5527.
[50] P. Flükiger, H.P. Lüthi, S. Portmann, and J. Weber, *MOLEKEL 4.3* Swiss Center for Scientific Computing, Manno. Switzerland, 2000–2002.
[51] S. Portmann and H.P. Lüthi, *MOLEKEL:* an interactive molecular graphics tool, Chimia. 54 (2000), pp. 766–770.
[52] M.J. Frisch, G.W. Trucks, H.B. Schlegel, G.E. Scuseria, M.A. Robb, J.R. Cheeseman, J.A. Montgomery, Jr, T. Vreven, K.N. Kudin, J.C. Burant, J.M. Millam, S.S. Iyengar, J. Tomasi, V. Barone, B. Mennucci, M. Cossi, G. Scalmani, N. Rega, G.A. Petersson, H. Nakatsuji, M. Hada, M. Ehara, K. Toyota, R. Fukuda, J. Hasegawa, M. Ishida, T. Nakajima, Y. Honda, O. Kitao, H. Nakai, M. Klene, X. Li, J.E. Knox, H.P. Hratchian, J.B. Cross, C. Adamo, J. Jaramillo, R. Gomperts, R.E. Stratmann, O. Yazyev, A.J. Austin, R. Cammi, C. Pomelli, J.W. Ochterski, P.Y. Ayala, K. Morokuma, G.A. Voth, P. Salvador, J.J. Dannenberg, V.G. Zakrzewski, S. Dapprich, A.D. Daniels, M.C. Strain, O. Farkas, D.K. Malick, A.D. Rabuck, K. Raghavachari, J.B. Foresman, J.V. Ortiz, Q. Cui, A.G. Baboul, S. Clifford, J. Cioslowski, B.B. Stefanov, G. Liu, A. Liashenko, P. Piskorz, I. Komaromi, R.L. Martin, D.J. Fox, T. Keith, M.A. Al-Laham, C.Y. Peng, A. Nanayakkara, M. Challacombe, P.M.W. Gill, B. Johnson, W. Chen, M.W. Wong, C. Gonzalez, and J.A. Pople, *Gaussian 03*, Revision B.03, Gaussian, Inc., Pittsburgh PA, 2003.
[53] R.F.W. Bader, *Atoms in Molecules, A quantum Theory; International Series of Monographs in Chemistry*, Oxford University Press: Oxford, U.K., 1990, p. 22.
[54] F. Biegler-König, J. Schönbohm, R. Derdau, D. Bayles, and R.F.W. Bader, *AIM 2000*, Version 1, 2000.